



Research Article

Design Optimization of Cessna 172 Wing With Biomimetic Design Approach

Hüdayim Başak ^{a*} Anıl Akdemir ^b ^a Department of Industrial Design Engineering, Gazi University, Ankara, Turkey^b Graduate School of Natural and Applied Sciences, Gazi University, Ankara, Türkiye

Article Info

ABSTRACT

Article history

Received: 26/02/2024

Revised: 25/03/2024

Accepted: 11/05/2024

Keywords:

*Biomimetics,
Wing Design,
Wing Cross-Section,
Flow Analysis.*

While the aircraft is moving in the opposite direction of the flow in the air, the wind resistance and the moment effect due to this resistance negatively affect the flight performance. In design studies, it is aimed to increase aerodynamic performance by minimizing these two negative factors. In this study, the effect of wing cross section and three-dimensional airfoil on aerodynamic performance is investigated numerically. Within the scope of this study, to reach the intended design, biomimetic design approach was used and new-wing designs were created to mimic the bird species' wings, which have the highest aerodynamic performance in nature. Based on the literature search for two-dimensional wing section selection, it was seen that the most preferred sections were identified and compared with the wing section of the Cessna 172 aircraft (NACA2412) in flow analysis. In the flow analysis conducted in the XFLR5 program, the aerodynamic performances of the wing sections at Reynolds value and angle of attack were investigated. According to this analysis, the aerodynamic efficiency of the NACA2412 section was higher than that of the other sections. In the three-dimensional flow analysis, biomimetic wing designs and the wing of the Cessna 172 aircraft were examined in the XFLR5 program at a cruising speed and angle of attack. It was observed that the aerodynamic efficiency of the wing design, which is inspired by the albatross, is higher than the other designs. Owing to the flow analysis, the albatross wing design provided 6.26% improvement in the lift coefficient, 15.73% in drag coefficient and 15.16% improvement in the glide ratio compared to the Cessna 172 aircraft wing design. For structural analysis, the pressure values obtained from the flow analysis results were used as the load distribution on the wing. In the designs created using the same material, it was observed that the weight of the wing inspired by the albatross was 34.156% less weight and 50.902% less deformation value obtained compared to Cessna 172 aircraft.

1. Introduction

The design process of the aircraft directly effects critical flight functions such as cruising distance, speed, flight comfort, number of passengers or cargo it can carry, altitude, operational space and maneuverability [1, 2]. All these components effect the fuel consumption [3] finally which is directly effected by the geometry of the wing [4]. There are many factors that must be considered during the design of the wing, such as the selection of two-dimensional section, aspect ratio, sharpness ratio, dihedral angle value, arrow angle and twist angle [5]. Each of these factors makes serious differences in the performance of the final wing design. Therefore, a designer must optimize several wing geometry parameters to obtain an efficient wing geometry that meets the design requirements. For this purpose, design studies in today's aviation world continue to be inspired from living creatures that can fly [6]. Flying creatures have the ability to make good use of the aerodynamic structure of their wings with the fluid resistance created by the wind and the sea and to travel kilometers with very little flapping of their wings and therefore with minimum energy consumption owing to their flight abilities, such as flying at very low speeds, gliding through the air, making sharp turns and flying backwards [7-9]. These abilities observed in nature are exemplary in the design stages, problem solving and finding new ideas in the field of aviation. When bird wings are

examined, we can see that there are two solution approaches to be applied in aviation: a movable structure like a bird's wing and a structure in the form of a bird's wing. However, since the movable structures are not suitable for the application, the form of the bird wing is inspired [10].

In the literature, biomimetic-based aviation vehicle designs are frequently encountered. Oo examined the structure of pigeons' the wing geometry at different angles to the forward and backward, after this examination he designed a wing geometry with a similar geometry. Considering these studies, it was seen that optimum results are obtained when the values of 20° backwards and 17.5° forwards are used together in wing design [10]. Upasena et al. studied the wing structure of Frigate birds and observed that the backward angle of the wing provides this bird species with high-gliding ability in long distance flights. While using this wing structure in the three-dimensional wing drawing, NACA-4412 airfoil was chosen for the two-dimensional section. In analyzes conducted between -16° and 30° angle of attack, he indicates that this design provides a high-lift-to-wind resistance ratio and low wing load [11].

In the study of Focke et al., the flying fish structure was taken as an example in the small-scale aircraft design. NACA 2806 was used on the front wing and NACA 0006 was used on the tail wing. When the analysis results close to sea level are compared with other heights, the lift coefficient value increased by 24.5% while the wind resistance coefficient value decreased by 1.56% [12].

*Corresponding author: Hüdayim Başak

*E-mail address: hbasak@gazi.edu.tr

<https://doi.org/10.56158/jpte.2024.66.3.01>

Sevillano et al. designed a grided structure similar to the wing tip of the vehicle they created by being influenced by the swirl structure on the wing tips of the birds. In the assumed operation with a Reynolds number of 5×10^4 and a flow rate of 10 ms^{-1} , the angle of attack was investigated only at 0° . According to the analysis results, 3% improvement in take-off speed and 12.5% decrease in the wind resistance coefficient were observed in the grid geometry [13].

The wing design inspired by the form found in the fins of the Humpback Whale was compared with the standard wing design. NACA0020 cross section was used in both wing designs. Solidworks program was used in the design and analysis process. As a result of CFD analysis at different speed values on these designs; the temperature, speed and pressure data on the wings were compared. These parameters were compared in terms of percentage efficiency ratios. In the findings obtained, the design with the humpback whale fin form showed higher efficiency in all parameters compared to the standard wing design. It is also concluded that materials with less strength and weight can be used in this design since less stress occurs in this design compared to the standard design [14].

Nithiyapathi et al. designed wing structures of northern tern, white pelican, rock eagle and albatross birds for biomimetic-based unmanned aerial vehicle wing design and compared them in terms of aerodynamic performance. NACA 4412, NACA 2412, NACA 23012, NACA 0012, NACA 0012, NACA 0006, MH60 and GOE 174 wing types, which are most commonly encountered in literature researches as two-dimensional wing sections, were examined in two-dimensional flow analysis with the help of XFLR5 program. The Reynolds number was assumed to be 5×10^4 and the aerodynamic performance of the wings was analyzed at angles of attack between 2° and 8° . As a result of the analysis, it was decided to use GOE 174 as a wing section since it showed the best performance. For three-dimensional testing, the wing structures of northern tern, white pelican, rock eagle and albatross were designed with XFLR5 and Solidworks programs. XFLR5 and Ansys programs were used for analysis. In order to compare the designs under the same conditions, wing lengths and wing areas were kept at the same values. The lift coefficient/wind resistance coefficient ratio was used as a comparison parameter. As a result of the analysis at 15 m/s flow velocity, the wing structure of the albatross bird offered the best performance among the bird species mentioned. According to this performance, the maximum lift coefficient value was reached at 6° and 8° angles of attack. Aydın et al. [17] examined the wing section design inspired by the shape of the maple seed. In the flow analysis performed at 3° and 30° angle of attack, it was seen that the stall angle of the wing had a high value of 23° . Additionally, it was observed that the lift coefficient was 2.33 and the wind resistance coefficient was 0.983 when the wing was at this angle. Park et al. [18] investigated the aerodynamic performance of the wing model, which was designed based on the floating swallowtail of butterflies. NACA0024 was chosen as the wing section. In the analyzes conducted at 5 ms^{-1} speed, it was observed that the L/D ratio reached the highest value at 5° attack angle [15].

Bektaş et al. designed the wings in Solidworks program inspired by the wing structure of bumblebee and sphinx butterfly and subjected them to flow analysis and static analysis with the help of Ansys program. In order to make comparisons in the analysis, different materials were tried and the results were observed. In addition, the effect of the number of meshes on the analysis was also examined by comparing different mesh structures. The flow test results were compared with wind tunnel test results obtained from different sources and their convergence was visualized on the graph. As a result of the flow analysis at different angles of attack, the maximum CL/CD ratio was reached at 5° angle of attack for both blade types. The angle

of attack at which the maximum lift coefficients were observed was 40° for the bumblebee and 30° for the sphinx butterfly. It was also observed that the lift coefficients were zero at 0° for both wing types. The wind resistance coefficient increased in direct proportion to the increase in the angle of attack between 0° and 90° and reached its maximum value at 90° . In the flow analysis, the amount of deformation at the wing tips was examined as a result of static tests at 5° angle of attack, which gave the maximum flow data value [16].

Aydın et al., investigated the wing section design inspired by the shape of a maple seed. They transferred the seed sample they found from nature to the ANSYS program via a three-dimensional scanner. Again, they created a two-dimensional airfoil design inspired by this seed section. In the flow analysis performed at 3° and 30° angle of attack values, it was observed that the stall angle of the wing had a high value of 23° . It was also observed that the lift coefficient was 2.33 and the wind resistance coefficient was 0.983 at this angle. The glide ratio (lift resistance / wind resistance) reached its maximum value at a blade angle of 5 degrees [17].

While the wing generates lift during flight, it also generates pitching moment, which prevents the airplane from flying in a stable manner, and drag force, which acts in the opposite direction to the wind direction of flight. These two factors negatively affect the aerodynamic performance of the airplane. In this study, biomimetics was used to minimize these negative aerodynamic factors and wing designs of living creatures in nature were used in wing designs. In addition, the effect of wing cross-section and three-dimensional airfoil on aerodynamic performance is numerically analyzed and the effect of wing shape on stress and deformation distribution on the wing is investigated.

2. Methodology

For the biomimetic-based wing design, flying creatures in nature were examined, and designs were made inspired by the wing structure of creatures with high aerodynamic efficiency. XFLR5 program was used for the design. The aerodynamic performance of the newly created design was analyzed with the help of Ansys Workbench program CFD (Computational Fluid Dynamics) analysis module and XFLR5 programs. Afterwards, its aerodynamic performance was compared with the Cessna 172 aircraft, which is already in use today. After examining and improving the flow performances, material selection was made for the newly designed part. In the process following the material selection, the effect of the high-pressure values formed at certain angles of attack on the wing was analyzed through the Ansys structural analysis module. At the end of the analysis, it was observed whether the strength of the part was sufficient or not.

2.1. Reference wing area

In this part of the study, reference wing models were analyzed to compare the biomimetic wing design with a current aircraft wing, the wing dimensions and flight conditions of the type Cessna 172 aircraft were obtained by analysis. Table 1 shows the dimensions of the wing structure and flight information of the aircraft.

2.2. Wing section (airfoil) selection

The wing section is as important a design parameter as the wing surface area. The wing section is responsible for producing the optimum pressure distribution in the upper and lower parts of the wing to generate the required lift for flight. To make the wing section selection, aerodynamic effects on the wing should be examined. For this reason, the factors affecting the wing aerodynamics and flow analysis methods were analyzed before the section selection.

Table 1. Wing dimensions of the Cessna 172 aircraft [19]

Wing Section	NACA2412
Wing Length	11 m
Body Wing Width	1,63 m
Wing Tip Width	1,13 m
Dihedral	1,7°
Aspect Ratio	7,5
Cruise Speed	63 m/s
Air Density	1,007 kg/m ³
Viscosity Value of the Air	1,714x10 ⁻⁵ m ² /s

2.2.1. Wing Aerodynamics

As an airfoil moves through the air, it generates an aerodynamic force backwards at a certain angle with the relative direction of travel. The force component parallel to the relative motion direction of this aerodynamic force is defined as the “drag force (D)” and the vertical force component is defined as the “lift force (L)” [20].

The lift and drag forces on the wing are defined as shown in Eq. 1 and Eq. 2 respectively. The moment in the horizontal plane created by the wing against the wind resistance during flight is defined as the pitching moment (M). Pitching moment on the wing is expressed as shown in Eq. 3.

$$L = \frac{1}{2} \rho A v_{\infty}^2 (C_L) \quad (1)$$

$$D = \frac{1}{2} \rho A v_{\infty}^2 (C_D) \quad (2)$$

$$M = \frac{1}{2} \rho A v_{\infty}^2 (C_M) \quad (3)$$

ρ is the density of the air (kg/m³), A is the surface area (m²), v_{∞} is the air flow velocity (m/s), C_L is the unmeasured lift coefficient, C_D is the unmeasured drag coefficient, and C_M is the unmeasured moment coefficient.

Glide ratio, is the ratio between the lift and drag forces or coefficients of the wing, as shown in Eq. 4 It is also the ratio of the distance traveled horizontally in a given time to the altitude loss [21]. For example, a glider with a glide ratio of 5 can have a range of 5 km when it starts flying from an altitude of 1 km. For this reason, the glide ratio value is critical in comparing the aerodynamic performance of aircraft.

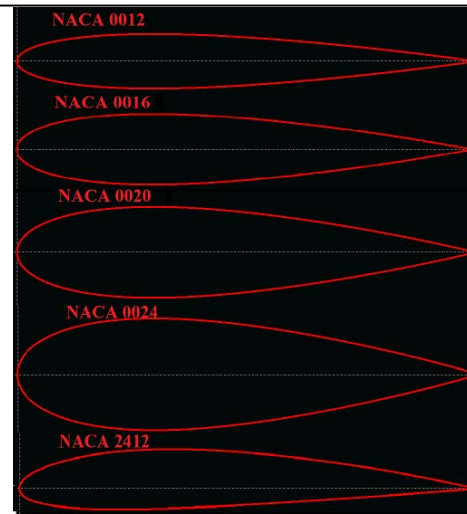
$$E = \frac{L}{D} = \frac{C_L}{C_D} \quad (4)$$

The angle between the direction of wind flow and the centerline of the airplane wing is called the "Angle of Attack." This angle has a great influence on the lift generated by the wing. As the angle of attack increases, the lift coefficient (C_L) and drag coefficient (C_D) acting on the wing increase in direct proportion. At low angles of attack, the airflow at the top of the wing flows smoothly. After a certain angle, the air flow starts to separate from the upper surface of the wing and a vortex flow is formed on the wing. This angle is called the "stall angle" [22].

2.2.2. Two-Dimensional Flow Analysis Method

Within the scope of wing drawing and flow analysis XFLR5 Program was used. The program can calculate and compare the lift coefficient, drag coefficient, pitching moment, pressure coefficients of airfoils in two-dimensional and three-dimensional analyses.

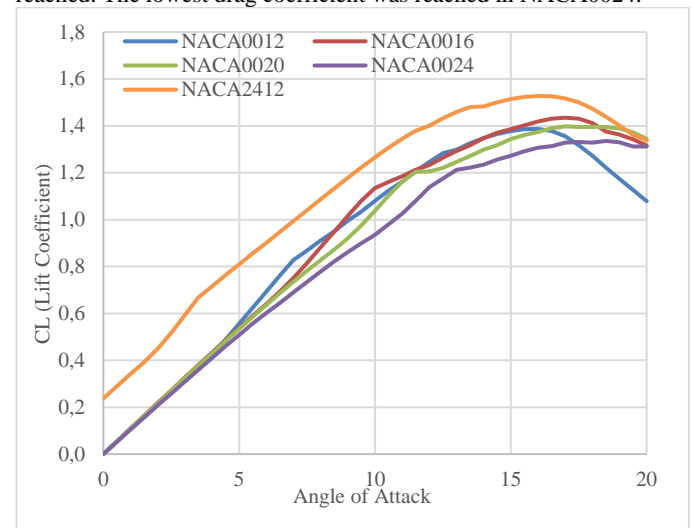
For the wing cross-section and flow analysis, the wing cross-section of the Cessna 172 (NACA2412) aircraft model was compared with the wing cross-sections with high aerodynamic efficiency (NACA0012, NACA0016, NACA0020, NACA0024 and NACA2412) in the literature [22]. The batch analysis module was used for two-dimensional wing analysis in the XFLR5 program. In the flow analysis performed at 106 Reynolds, the aerodynamic performances of the wings were investigated between 0° and 20° angle of attack. The drawings of the sections are visualized in Figure 1.

**Fig.1** Drawings of wing sections

2.2.3. Comparison of Lift and Drag Coefficient of Wing Sections

Figure 2 and 3 show graphs of the lift coefficient and drag coefficients with respect to the angle of attack for all airfoils. When the angle of attack is 0°, the lift coefficient value of the NACA2412 airfoil is 0.21, while the lift coefficient value of the other wing types are 0. While the angle of attack increased between 0° and 16°, the lift coefficient value increased in all airfoils. The lift coefficient started to decrease in NACA0012 at 16°, NACA0016, and NACA2412 at 17°, and NACA0020 and NACA0024 at 18°, respectively. These angle values refer to the stall angle (the situation where the air flow above the wing breaks off from the wing surface) of the wings. The NACA2412 has higher lift coefficient values at all angles of attack and its stall angle was better than other wings.

We observed that the drag coefficient value was greater than 0 in all wing types at 0° angle of attack and its value increased as the angle of attack value increased. We observed that the drag coefficient increased much more rapidly after the stall angle was reached. The lowest drag coefficient was reached in NACA0024.

**Fig. 2.** Comparison of lift coefficient for airfoils

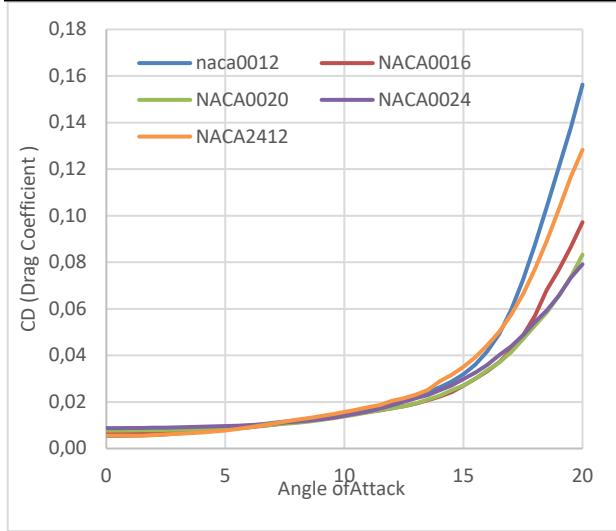


Fig. 3. Comparison of drag coefficient for airfoils

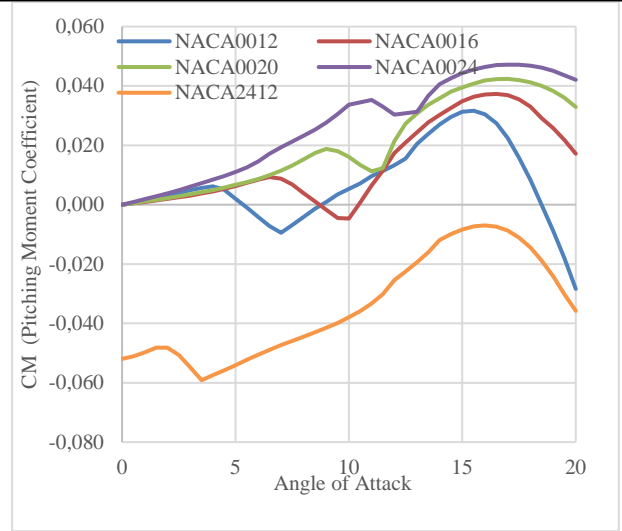


Fig. 4. Comparison of pitching moment coefficient for airfoils

2.2.4. Comparison of the Glide Ratio and Pitching

Moment Coefficient of Wing Sections

During flight, the front part of the aircraft wants to turn with a backward moment due to wind resistance. To prevent this, the pitching moment (CM) value for mid-wing aircraft should be negative and close to zero. If these conditions are fulfilled, an m is created with the nose of the plane down. In the overhead wing structure, the center of gravity of the aircraft is higher than that in the middle or lower wing type. Additionally, the overhead wing aircraft are subject to greater drag. Therefore, the CM value should have a greater negative value for upper-wing aircraft than for mid-wing aircraft. Figure 4 shows the CM values of the wings at different angles of attack. The CM value of the NACA2412 wing type has a larger negative value than that of other wing types. Therefore, it was concluded that this wing type is more suitable for overhead wing aircraft design.

Figure 5, the ratio of lift coefficients to drag coefficients (CL/CD), ie glide ratio, is examined at different angles of attack of the wings. For wings, this ratio is the most important parameter that shows the aerodynamic efficiency of the wing. The higher this ratio, the more distance the aircraft can travel in the horizontal plane. The glide ratio of all wing types increased with the increase in the angle of attack and started to decrease after a certain point. At 0° angle of attack, all wing types have a glide ratio value of approximately 0, while the NACA2412 has a value of 42 (Figure 5). At all angles of attack, this wing type has a higher glide ratio than other wing types. It is seen that the NACA2412 wing type achieves maximum aerodynamic efficiency when the angle of attack is at 5°.

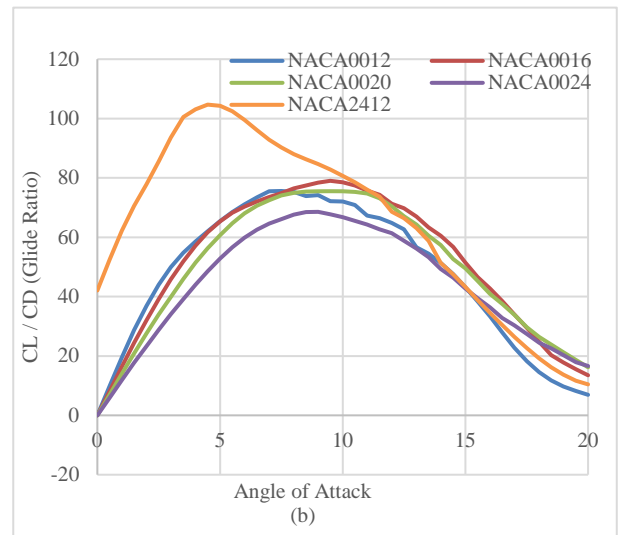


Fig. 5. Comparison of glide ratio for airfoils

Table 2. Parameters to be used in the design [22]

Number of Wings	1
Kanadın Dikey Pozisyonu	Upper Wing
Vertical Position of the Wing	NACA 2412
Wing Span Rate	7,5
Dihedral Angle	1,7°
Arrow Angle	0°
Twist Angle	0°
Winglet Usage	Yok
Wing Length	11 m

2.2.5. Modeling of Cessna 172 aircraft wing

In this part of the study, the wing structures of bird species in nature are imitated by using the biomimetic science branch and the design process is created using the XFLR5 program. In addition, the wing structure of the Cessna 172 aircraft type, which was used as the reference aircraft wing structure in the study, was also modeled. Table 2. visualizes the dimensions used for drawing the Cessna 172 aircraft wing in the XFLR5 program. The aircraft wing length is 11m long. "Chord" value is the distance between the head and the tip of the wing section (table 3). The "Dihedral" value has a value of 1.7° in the Cessna 172 aircraft type, so this value was used. "Twist" is the twist angle, since this value is 0° in the Cessna 172 airplane wing design, the same design structure is used. In the "Foil" section, the wing section type is selected. Based

on the X and Y panel values, the values required for the network structure to be created in the analysis to be performed on the wing were entered. The three-dimensional wing design created according to the entered values is given in Figure 6.

Table 3. Dimensions used in wing drawing of Cessna 172 airplane

Y(m)	Chord (m)	Offset (m)	Dihedral (°)	Twist (°)
0,000	1,630	0,000	1,7	0,00
1,340	1,630	0,000	1,7	0,00
2,680	1,630	0,000	1,7	0,00
4,090	1,380	0,075	1,7	0,00
4,795	1,225	0,112	1,7	0,00
5,500	1,130	0,150	1,7	0,00

Foil	X-panels	X-dist	Y-Panels	Y-dist
2412	20	Cosine	5	Sine
2412	20	Cosine	5	Sine
2412	20	Cosine	5	Sine
2412	20	Cosine	5	Sine

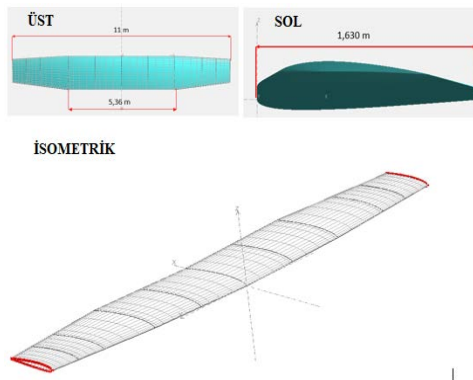


Fig. 6. Modeling of Cessna 172 aircraft wing pattern in XFLR5 program

2.3. Biomimetic Design of the Wing

Biomimetic design methodology is applied to understand the principles of fundamental mechanisms in nature and to use these structures as solutions to engineering problems. From the past to the present, human beings have benefited from the findings observed from nature in most of the inventions or in the complex engineering problems for which they seek solutions. Biomimetics embraces the idea that there is no better example than nature for developing something new or for solving engineering problems. Additionally, it is a realistic approach to imitate the structure of nature to find more environmentally and friendly solutions.

Designs inspired by birds contribute the development of the aviation industry from the past to the present. The aim of this study, designing a wing with high lift and low drag. For this reason, living species with advanced aerodynamic structures in nature were investigated. In the literature research, the findings about aerodynamic structures of birds obtained by biologists were examined. The most important point to be compared between these findings is the glide ratio. Because this ratio shows how far living species can travel despite wind resistance and their aerodynamic performance characteristics. In Figure 7, glide ratio values of bird species with the highest aerodynamic performance in nature are shown [23]. According to Figure 7, biomimetic designs were created inspired by the wing structures of four bird species with the highest gliding rate, such as albatross, vulture, gull and pigeon.

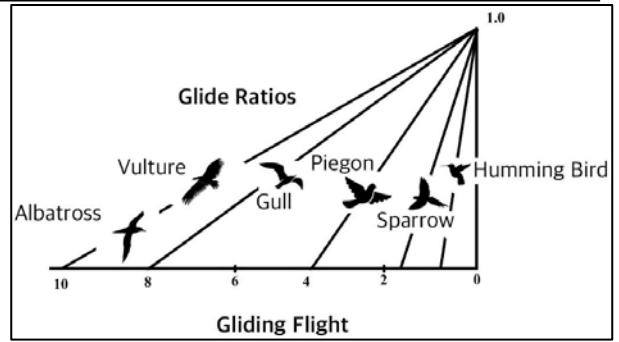


Fig. 7. Bird species according to glide ratios [23]

In the XFLR program, biomimetic-based wing designs were realized with the same methods used in Cessna 172 aircraft wing modeling. Figure 8 show the designs created by simulating the wing structure of albatross, vulture, gull and pigeon bird species according to the wing spread pictures. Similar wingspan, wing length, wing cross section, twist angle and dihedral angle were used with the Cessna 172 airplane wing used as a reference in the study.

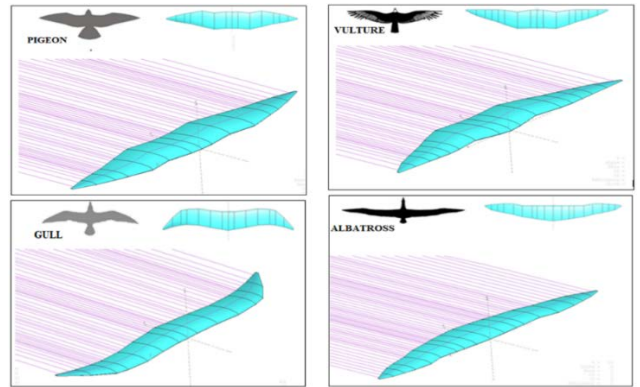


Fig. 8. Wing design inspired by the wings of gulls

3. Results

There are three different methods for flow analysis in XFLR5 environment. These methods are LLT, VLM and 3D panel method respectively. These methods have their own advantages and disadvantages in flow analysis. The LLT method analyzes the flow in the XY plane. Therefore, while this method can be used on wings with elliptical or flat geometry, it cannot be used on wing types with low wingspan, arrow angle and delta type. The LLT method gives reliable results at high angles of attack and stall angle. The VLM method, which was developed for the limitations of the LLT analysis type, can be used for all wing geometry types, low span ratios and high arrow angles. Another difference of the VLM method from the LLT method is that it includes the blade speed and the viscosity of the air in the analysis. The disadvantage of the VLM method is that it can only be used at low angles of attack. This is because when calculating the air velocity and viscosity in the analysis, it cannot converge these values close to the stall angle. The VLM method examines the aerodynamic performance along the wing section and gives realistic results. The 3D panel method, on the other hand, takes into account the thickness of the wings and is used in designs that include the analysis of the fuselage along with the wings. Thanks to this method, pressure distributions on the upper and lower surfaces of the wings can be observed with closer results [26].

The VLM (Vortex lattice method) method was used in the flow analyzes performed in the XFLR5 program. For analysis condition, flow rate 63ms-1, density 0.996 kgm-3 and dynamic density 1.74 x 10-5m2s-1 were chosen as the analysis inputs. Wing designs were analyzed in the range of -8° to 8° angle of attack. In the airfoil selection process, only airfoil geometry or pressure distribution is not considered. In addition to these, some

graphs showing the operational outputs of the airfoil, which are more informative about aerodynamic performance and flight stability, are analyzed to meet the design requirements [18]. These graphs are essentially variations of the lift, drag, and pitching moment coefficients and the glide ratio with respect to the angle of attack.

3.1. Comparison of Lift Coefficient and Drag Coefficient of

Wing Profiles

The designs with albatross, gull, pigeon and vulture wing geometries inspired by bird species in nature and the wing structure of the Cessna 172 aircraft are compared in Fig. 9 according to the lift coefficient (CL). We observed that the lift coefficient increases in direct proportion as the angle of attack increases. It has been observed that the lift coefficient has a positive value when the angle of attack is 0° in all wing types. The lift coefficients of the wing design reached their maximum values when the angle of attack was 8°. At this angle of attack value, albatross, gull, pigeon, vulture and Cessna 172 wings reached lift coefficient values of 0.890286; 0.872116; 0.8284655; 0.8170196; 0.8377896, respectively. As it is understood from the values, the albatross wing structure provided the highest aerodynamic performance according to the lift coefficient value. In addition, albatross and gull wing structures have higher lift coefficient values than the lift coefficient of the reference aircraft type, while pigeon and vulture wings have lower lift coefficient values. As can be seen from the values, the albatross wing structure provided the highest aerodynamic performance according to the lift coefficient value.

The drag coefficients (CD) of the biomimetic designs and the wing structure of the reference aircraft depending on the angle of attack are compared in Fig. 10. The design with the lowest drag coefficient is the one with the highest aerodynamic efficiency. While the drag coefficients of the designs showed close values between -8° and 0° angle of attack values, they showed different values between 0° and +8°. The differences in the drag coefficients of the wing designs were observed more clearly at the 8° angle of attack. At this angle of attack value, albatross, gull, pigeon, vulture and Cessna 172 wings reached drag coefficient values of 0.03179765; 0.03378288; 0.03368016; 0.03368016; 0.03277768; 0.0368023, respectively. All of the biomimetic wing designs performed better than the Cessna 172 aircraft wing type when compared according to the drag coefficient value. In addition, as in the lift coefficient value, it was also observed that the design created by resembling the wing of the albatross bird in the drag coefficient values offered better aerodynamic performance than the other wing designs.

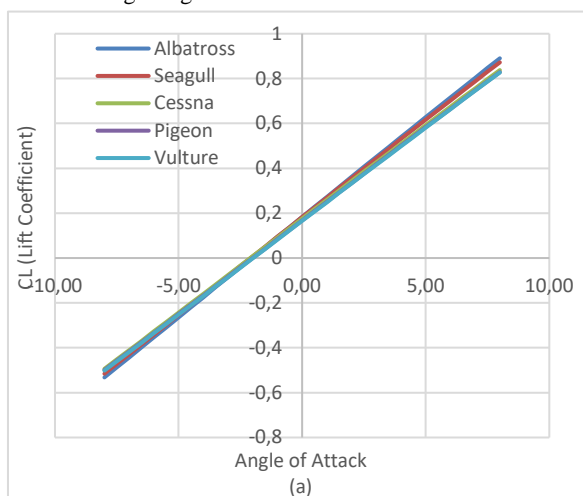


Fig. 9. Comparison of lift coefficient for wing profiles

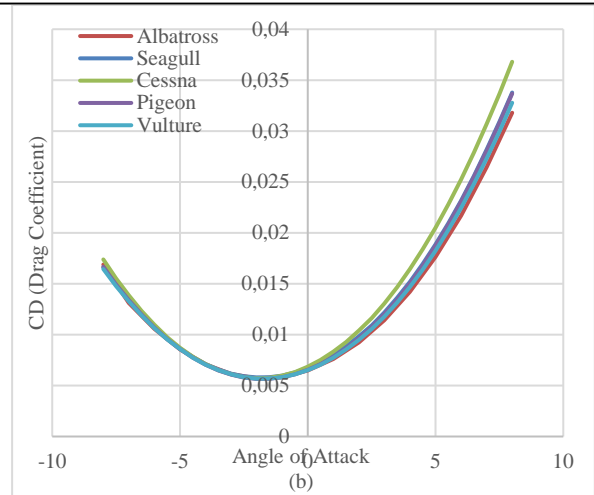


Fig. 10. Comparison of drag coefficient for wing profiles

3.2. Comparison of The Glide Ratio and Pitching

Moment of Wing Profiles

The glide ratios (CL/CD) bio-inspired wing structures of the Cessna 172 aircraft are shown in Fig. 11. The glide ratio is the most important parameter that shows the aerodynamic performance of a wing design. In comparison, Cessna 172 aircraft wing has a higher glide ratio in the range of -8° to -4° angle of attack. In the range of -4° to 8° angle of attack, biomimetic wing designs offered higher performance. Additionally, on this angle of attack range, the glide ratio value of the albatross wing structure showed a better aerodynamic performance compared with other wing types.

If the pitching moment coefficient is positive, the nose of the airplane tends to move upwards. In the case of negative, the nose of the plane tends to move downwards. Therefore, for stable flight, when the angle of attack is zero degrees, the coefficient of pitching moment should have a negative value and be close to zero. The comparison of the pitch moment coefficients (CM) of the designed wings is visualized in Fig. 12. When the angle of attack was 0°; Pitching moment coefficients of the wings of albatross, gull, pigeon, vulture and Cessna 172 were by order; -0,1978113; -0,2336351; -0,2405375; -0,2616895 and -0,2743365. Since its pitch moment coefficient is negative and closer to the zero value, It has been observed that the flight balance of the albatross wing structure is more stable than the others are.

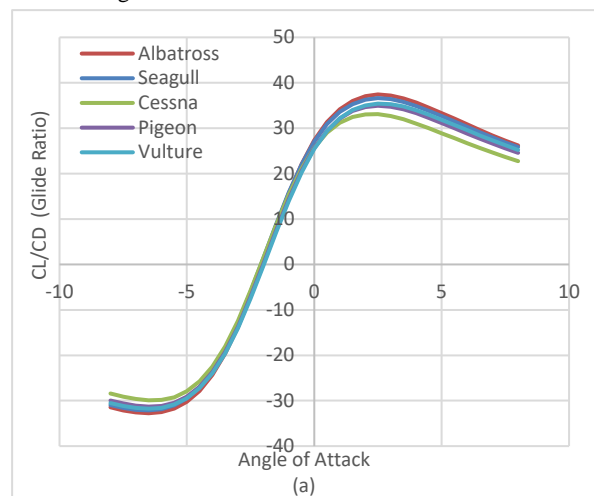


Fig. 1. Comparison of glide ratio for airfoils

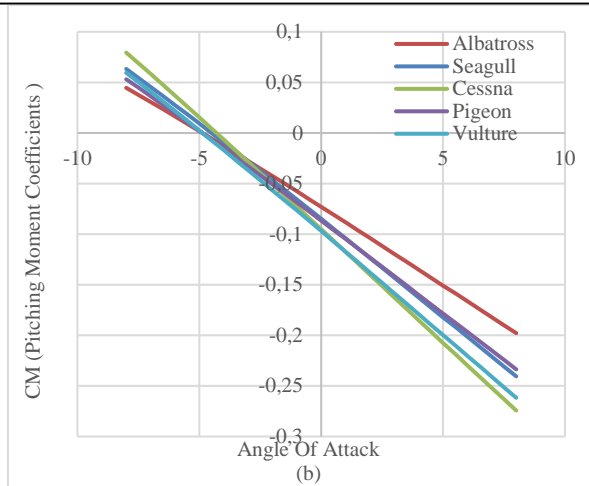


Fig. 2. Comparison of pitching moment coefficient for airfoils

4. DISCUSSION

Three-dimensional models of the wing structures were created with the help of XFLR5 program. These models are given in Figures 6 and 8. While obtaining the three-dimensional models of the wing structures, firstly, the Cessna 172 aircraft wing, which will be used for comparison, was modeled in 1/1 scale. Then, the wing models of the bird species given in Figure 8 were modeled in the same dimensions as the Cessna 172 model, reflecting only the changes in the wing geometry.

The rib structure is the structural element of the wings. It ensures that the wing maintains its shape in case of excessive load and transfers the pressures formed on the wing to the spar. Surfaces were added to the designed two-dimensional section geometries, thickness was assigned to these surfaces, and the rib structure of the wing was created. Holes are drilled on them to reduce the weight of the wing. The connections of the ribs were provided by the spar design. Fig. 13a. shows rib and spar design of the wing.

The outer geometry of the wing was created by combining the surface geometries of the designed ribs with the 'Skin' command. With the 'Enclosure' command, a rectangular structure covering the wing was created. The created wing geometry and the rectangular structure covering are visualized in Fig. 13b. in order to define this design structure in the flow analysis, the front surface of the rectangle is defined as the 'air inlet', the rear surface as the 'air outlet', the wing geometry as the 'main body' and the remaining surfaces of the rectangular geometry as the 'walls.' After the design process, the mesh structure should be created to prepare for the analysis environment. In the analysis conducted over the skewness value to examine the mesh quality, it was observed that the maximum skewness value of the mesh structure created using the 461765 mesh element was 0.78. According to the mesh skewness table which is shown in Fig. 13c, it was seen that the maximum skewness value was at a good level.

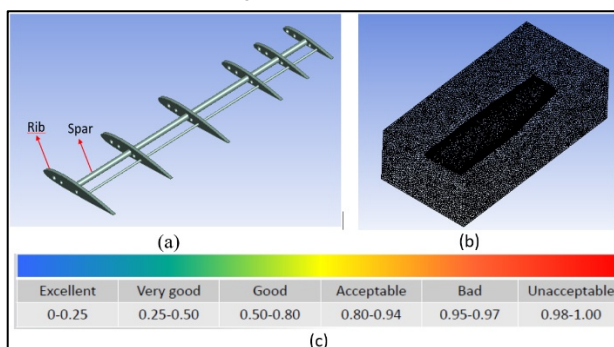


Fig. 3. Wing design (a) rib and spar (b) mesh structure (c) mesh skewness table

While creating the analysis conditions, the sin (8°) and cos (8°) values, which are the equivalent of 63 ms-1, which is the cruise speed of the Cessna 172 aircraft, at the 8° angle of attack were taken as reference. Additionally, the density of the flow is 0.996 kgm-3 and its dynamic density is 1.74 e-05 m2s-1 in the analysis inputs. The pressure distribution on the wing is shown in Fig. 14a. The maximum pressure value was 2481,48 Pa and it was formed in the front region of the wing. Because the front part of the wing is the part that first encounters the air flow. Due to the large curved surface at the front of the wing, the airflow slows down for a short time before flowing to the rear parts of the wing, causing high pressure. The lowest pressure value occurs at the rear end of the wing. Different pressure values occurring at different points of the wing will be used as a source for the load information on the wing in the static analysis. For static analysis, the first wing structure created during the flow analysis was redrawn. Aluminum material, which is the wing material of Cessna 172 aircraft, was chosen for the material assignment. We observed that the weight of the wing after the assigned material was 2876,8 kg. The mesh structure has been reconstructed for the wing. For the static analysis conditions, the pressure values on the wing were taken from the flow analysis results. Additionally, the area indicated by the symbol B in Fig. 14b. is the surface where the wing and fuselage meet, and this surface is fixed. Gravity, indicated by the symbol A, has also been added to the analysis conditions to obtain realistic results.

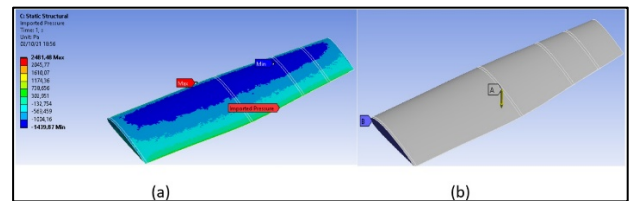


Fig. 4. Preliminary to analysis (a) pressure distribution (b) analysis conditions

To examine the static analysis results, the total deformation, maximum stress and Von-Mises stress values were added to the analysis conditions in the analysis results. The deformation on the wing due to the pressure distribution obtained according to the flow analysis results is shown in Fig. 15a. We observed that the maximum deformation of the wing was 12,412 mm at the wing tip. Moreover, in the region where the wing connects to the fuselage, the deformation is minimal. Fig. 15b. Von-Mises stress values formed on the wing are visualized. The maximum Von-Mises stress value was 17,525 MPa, and it occurred at the junction of the wing and fuselage. The maximum stress value was 27.51 MPa, as shown in Fig. 15c. As observed in the Von-Mises stress value, the maximum stress value reached the maximum value at the junction of the wing and fuselage.

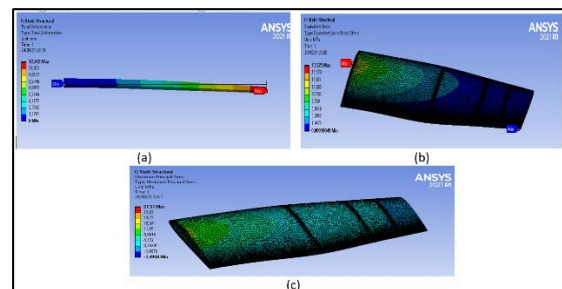


Fig. 5. Analysis results of Cessna 172 (a) total deformation (b) Von-Mises stress (c) maximum stress

The design, flow analysis and static analysis studies of the Cessna 172 aircraft wing in the Ansys program were also applied to the albatross wing structure. To make comparisons, aluminum material type is used in material definition. With the use of aluminum material, the weight of the geometry was 1894,2 kg. Fig. 16a. shows the pressure distribution on the albatross wing type. The maximum pressure formed is 2178,9 Pa and reached its

maximum value in the front part of the wing, as in the wings of Cessna 172 aircraft. The minimum pressure value also occurred at the tip of the wing, as in other wing types.

In Fig. 16b, the deformation values caused by the pressure values formed on the wing can be seen. The maximum deformation was 6,094 mm, and it occurred in the tip region of the wing, as in the wing design of the Cessna 172 aircraft. The maximum stresses on the wing are shown in Fig. 16c. The maximum stress in the wing root region is 7,413 MPa. Maximum Von-Mises stress values are shown in Fig. 16d. This maximum Von-Mises stress in the root region of the wing is 5,2126 MPa. The minimum Von-Mises stress occurred at the tip of the wing.

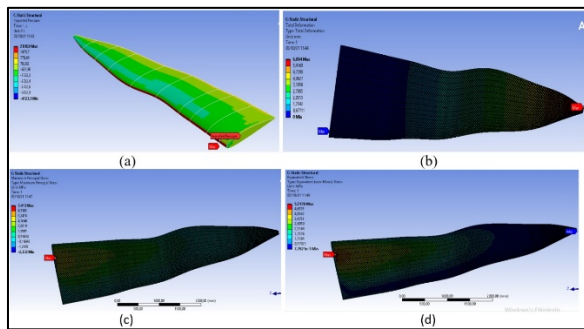


Fig. 6. Analysis result (a) pressure distribution (b) total deformation (c) maximum stress (d) Von-Mises stress

The wing structures of the albatross and Cessna 172 aircraft are compared according to the static analysis results (Table 3). With the Albatross wing design, the wing weight, maximum pressure, maximum deformation, maximum Von-Mises stress, and maximum stress values improved by 34,156%, 12,193%, 50,902%, 70,256%, and 73,053%, respectively, as indicated in the table.

Table 3. Comparison of static analysis results of wings

	Cessna 172 Wing	Albatross Wing	Improvement
Weight (kg)	2876,8	1894,2	% 34,156
Maximum pressure value (Pa)	2481,4	2178,9	% 12,193
Maximum deformation value (mm)	12,412	6,094	% 50,902
Maximum Von-Mises Stress Value (MPa)	17,525	5,2126	% 70,256
Maximum stress value (MPa)	27,51	7,413	% 73,053

5. Conclusions

In this study, similar studies conducted in the past for selecting the airfoil, which is one of the most critical parameters in wing design, were examined and the airfoils with the highest aerodynamic performance were determined. To compare the aerodynamic performance of the designs made, the wing geometry of the Cessna 172 aircraft, which is still in use today, was taken as reference. At the end of the analysis, it was seen that NACA2412 had a higher glide rate than other airfoils have. It was also observed that the flight balance is more stable than other airfoils. After choosing the airfoil, new designs with similar dimensions were studied by taking the wing geometry of the Cessna 172 aircraft as a reference in the three-dimensional wing design by using biomimetic design methodology. The biomimetic wing designs created were inspired by the bird species gull, albatross, vulture and pigeon. To compare biomimetic designs among themselves and the wing of Cessna 172 in terms of aerodynamic performance, three-dimensional flow analysis was conducted in the XFLR5 program. It was observed that this wing structure provides

6.26% improvement in the lift coefficient, 15.73% in drag coefficient and 15.16% improvement in the glide ratio compared to the Cessna 172 aircraft wing. Flow analysis was conducted by using the CFD. The pressure values on the wing obtained from flow analysis were used as the load source for the static analysis. According to the findings obtained, it was observed that the weight of the albatross wing design was 34.156%, the maximum pressure value 12,193%, the maximum deformation value 50.902%, the maximum Von-Mises stress value 70.256% and the maximum tension value 73.053% less than the wing of the Cessna 172 aircraft.

Declaration of conflicting interests

The authors declare no competing interests.

Funding

The author received no financial support for the research and/or authorship of this article.

References

- [1] Torenbeek E., 2013, *Advanced aircraft design: conceptual design, analysis and optimization of subsonic civil airplanes*, 1st Edition, WILEY, USA, Newyork,
- [2] Gül I, Kolip A., 2018, *Performance of Production Special Section Profiles* El-Cezeri.; 5(3): 816-27.
- [3] Guerrero JE, Maestro D, Bottaro A. 2012, *Biomimetic spiroid winglets for lift and drag control*. Comptes Rendus Mécanique.; 340(1): 67-80.
- [4] Jentys MM, Effing T, Breitsamter C, Stumpf E. 2022, *Numerical analyses of a reference wing for combination of hybrid laminar flow control and variable camber*. CEAS Aeronautical Journal. 13(4): 989-1002.
- [5] Cevdet Ö, Özbek E, Ekici S., 2021, *A Review on applications and effects of morphing wing technology on UAVs*. International Journal of Aviation Science and Technology. 1(01): 30-40.
- [6] DeBlois MC., 2020, *Evolution of Sauropterygian Swimming Mode and Flipper Functional Morphology.*, Phd. Dissertation, University of California, USA.
- [7] Tobalske BW. 2007, *Biomechanics of bird flight*. Journal of Experimental Biology. 210(18): 3135-3146.
- [8] Abozeid S, Pokhrel S, Eisa S., 2023, *A Comprehensive Assessment to the Potential of Reinforcement Learning In Dynamic Soaring*. AIAA SCITECH, 23-27.
- [9] Zhang, H., & Liu, Z., 2022, *Design and Research on Flapping Mechanism of Biomimetic Albatross*. In Journal of Physics: Conference Series Vol. 2343, No. 1, p. 012006.
- [10] Oo, N.L. 2015, *Bionic Wing Design*, University of Hertfordshire.
- [11] Upasena, K. K. S. P., Weerathunga, U. I., Abeygoonewardena, J. I., & Bandara, R. M. P. S. 2019, *Design of a new aircraft wing inspired by the Magnificent Frigate bird*. International Research Conference Articles (Kdu Irc).
- [12] Focke, V. E., Kesel, A. B., & Baars, A., 2017, *Flying fish: Biomimetic potential for wing in ground effect crafts?* Innovationspotenziale für Technologieanwendungen. 8. Bremer Bionik-Kongress.
- [13] Bardera-Mora, R., Garcia-Magariño, A., Barroso, E., & Rodriguez-Sevillano, A. 2019. *Experimental Determination of Profile and Induced Drag Components in a Biomimetic Design MAV with Grids*. In AIAA Aviation 2019 Forum p. 3580.
- [14] Başak H, Demirhan H., 2017, *Examination of Wing Profile Yield Inspired by The Fins of Humpback Whale with CFD Analysis*. Gazi Journal of Engineering Sciences. 3(2): 15-20.
- [15] Nithiyapathi, C., Sreelakshmy, P. S., & Suman, M. 2021. *Aerodynamic Characterization of An Albatross Wing for Bio-Inspired Unmanned Aerial Vehicle*. Materials Today: Proceedings, 37, 1659-1664.
- [16] Bektaş, M., Güler, M. A., & Kurtuluş, D. F. 2020, *One-way FSI Analysis of Bio-Inspired Flapping Wings*. International Journal of Sustainable Aviation, 6(3), 172-194.
- [17] Aydın N, Karagöz İ, Çalışkan M. 2020, *A Study on A New Bio-Inspired Wing Design And 2D Analysis of Its Aerodynamic Characteristics*. Euroasia Journal of Mathematics, Engineering, Natural & Medical Sciences. 7(8): 126-136.
- [18] Park H, Bae K, Lee B, Jeon W-P, Choi H., 2010, *Aerodynamic performance of a gliding swallowtail butterfly wing model*. Experimental Mechanics, 50: 1313-21.
- [19] Jane, I., *All the World's Aircraft Dev&Production.*, IHS Global Ltd., 2018.

-
- [20] Bohara, K., Deepesh, D., Dhruva, A., Prajapati, K. 2019, *Performance Analysis of Airfoil Using Biomimicry: Serrated Trailing Edge and Denticles Inspired Surface*. John Wiley And Sons.
- [21] Eraslan, Y., 2018. *A training sailplane design*, Gaziantep Graduate School of Natural & Applied Sciences, master's thesis.
- [22] Sadraey, M. H. 2012, *Aircraft design: A systems engineering approach*. John Wiley & Sons.
- [23] Dhawan S. 1991, *Bird flight*. *Sadhana*, 16(4): 275-352.
- [24] Başak H., Akdemir, A., 2021., *Biomimetic-Based Aircraft Wing Design*, 6th International Engineering and Technology Management Congress, Turkey.
- [25] Gao, J., An, W., Shi, F., Wang, W., & Su, J. 2021, *The Influence of Wing Deformation on Energy Extraction During Dynamic Soaring*. In International Conference on Aerospace System Science and Engineering pp. 627-644.
- [26] Deperrois, A. 2009, *XFLR5 Analysis of foils and wings operating at low Reynolds numbers*. Guidelines for XFLR5, 142.